

# Ultra-fast sintering and grain boundary metastability in ceramics

Mattia Biesuz<sup>\*</sup> , Levent Karacasulu 

University of Trento, Department of Industrial Engineering, Via Sommarive 9, 38123 Trento, Italy

## ARTICLE INFO

### Keywords:

Sintering  
Ceramics  
Ultrafast high-temperature sintering  
Flash sintering  
Grain boundaries

## ABSTRACT

Grain boundaries (GB) are critical in polycrystalline ceramics. They control the material's properties as well as the diffusional processes. While they received little attention from the ceramics processing scientists for decades, the new developments in ultra-rapid sintering technologies (flash sintering, ultrafast high-temperature sintering, fast firing, photonic sintering...) have dramatically changed the context. Recently, it has been shown that rapid consolidation can be achieved in a timeframe shorter than that required for the interfaces to relax to their equilibrium state. This provides a detectable reduction in the activation energy for diffusion and sintering (about 8% in alumina), resulting in exceptional densification. Besides sintering, this result is of broader interest, as it provides a new approach to grain boundary engineering. In this short review, we discuss the current research context and outline future perspectives related to rapid sintering with a focus on its impact on the grain boundaries. New interpretations of non-conventional microstructures and scaling laws during rapid firing are also proposed based on the concept of grain boundary metastability.

## 1. Why grain boundary metastability matters?

Controlling processing conditions to tailor microstructures — and therefore material properties — is the cornerstone of materials engineering. Traditionally, property–processing–microstructure relations are studied at the microscale, focusing on the bulk 3D microstructure and often neglecting the effects of smaller-scale defects. Although point defects and grain boundaries (GB) are widely acknowledged as critical to polycrystal properties [1], systematic approaches to tailoring them through processing remain limited. This has been mostly driven by the idea that defects, excluding dislocations, are generally thought to be bound just to the chemistry, thus falling outside the primary interests of processing engineers.

Recently, a new concept related to grain boundary metastability in rapid, non-conventional sintering has emerged, opening new opportunities. These should be considered in a broad context that extends well beyond the sintering community itself. While metastable grain boundaries clearly influence densification kinetics and sintering, they can also significantly affect the final properties of the sintered polycrystal [2]. For example, the blocking effect of grain boundaries is a major challenge in ionic conductors [3,4]; tailoring the GB structure could also influence thermal transport properties [5] and, consequently, the thermoelectric figure of merit [6]. On these bases, the use of ultra-rapid sintering tools is expected to foster a shift in the “sintering optimization paradigm,”

which has traditionally focused solely on the correlation between density and grain size and processing parameters. In other words, a new optimization perspective can emerge, including the use of advanced sintering approaches to engineer interfaces and defects.

Besides being extremely attractive, some open questions remain about the possibility of grain boundary engineering via rapid sintering. The first issue is related to the temperature control in rapid sintering technologies, where temperature gradients can develop, thus leading to inhomogeneous microstructures and possibly inhomogeneous grain boundary states. A second question is related to the stability of these out-of-equilibrium features after sintering. Indeed, these will likely relax in systems that find application at high temperatures, but we trust they will remain in a large set of functional ceramics like thermoelectrics, dielectrics, and ionic conductors. Note that even if ionic conductivity is activated, this belongs to the movement of the fastest ion in the system, while grain boundary relaxation would require the rearrangement of the slowest species. Even in electrolytes operative at relatively high temperatures, like YSZ, the grain boundary metastability could be preserved for long times based on the high diffusion barrier for cations.

Nonetheless, some theoretical frameworks are still lacking, and the concept so far relies on only a few fragmented experimental observations. However, these results appear relatively robust and general. If supported by further experimental studies, we believe that the ability to consolidate materials with out-of-equilibrium grain boundaries through

<sup>\*</sup> Corresponding author.

E-mail addresses: [mattia.biesuz@unitn.it](mailto:mattia.biesuz@unitn.it) (M. Biesuz), [levent.karacasulu@unitn.it](mailto:levent.karacasulu@unitn.it) (L. Karacasulu).

<https://doi.org/10.1016/j.cossm.2026.101258>

Received 31 December 2025; Received in revised form 13 February 2026; Accepted 13 February 2026

Available online 25 February 2026

1359-0286/© 2026 The Author(s). Published by Elsevier Ltd. This is an open access article under the CC BY license (<http://creativecommons.org/licenses/by/4.0/>).

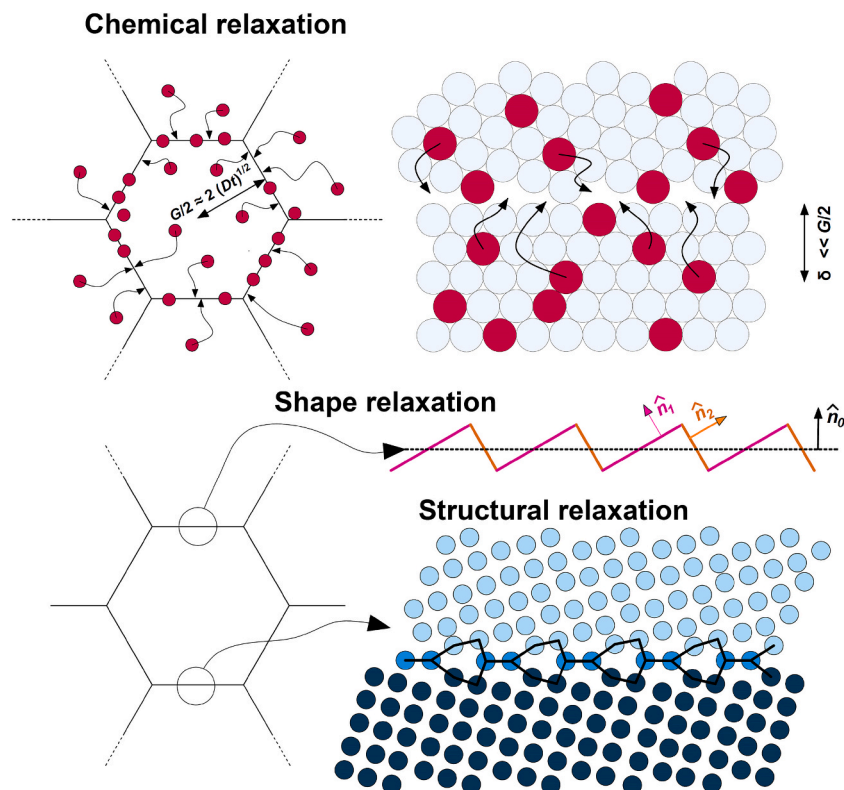


**Fig. 1.** Schematic representation of the possible relaxation phenomena occurring at the grain boundaries: (i) chemical relaxation involving dopants diffusion from the bulk of the grains (top left) or just on the GB vicinity (top right), these are governed by GB energy excess reduction induced by the Gibbs adsorption; (ii) shape relaxation due to the development of faceted boundaries along different low-energy crystallographic directions ( $n_1$  and  $n_2$ ); (iii) structural relaxation related to an ordering of the GB core providing a 2D-unit cell repeated in the GB plane.

non-conventional sintering could represent a breakthrough in ceramics processing science for the next decades. In this short manuscript, we aim to outline some theoretical aspects of grain boundary metastability, highlight the current context, and medium/long-term perspectives.

## 2. The context

To fully appreciate why grain boundary metastability matters related to sintering, we must first recall how heating rates impact the densification process.

The recent development of various ultra-rapid sintering techniques (fast firing-FF- [7], ultrafast high temperature sintering-UHS- [8,9], flash sintering-FS-[10], spark plasma sintering-SPS-[11,12], hybrid flash-SPS[13–16], microwave sintering–MWS-[17], photonic sintering [18,19]... [20,21]) has dramatically increased the interest regarding the interactions between heating rate, densification kinetics, and microstructural control. Beyond the analytical and numerical tools used to model ultrafast densification [22], the experimental approaches to study sintering in extreme conditions are quickly evolving with the development of ultrafast optical-dilatometry up to  $200^\circ\text{C min}^{-1}$ . [23].

There has been a long discussion about whether and how much the heating rate can impact densification, with scattered conclusions [24–30]. This is largely because many rapid sintering technologies employ electric fields and currents; therefore, it is not easy to decouple field/current-induced phenomena (electromigration[31,32], ponderomotive forces [33], electrochemical reductions [34–36]...) from effects solely relying on the heating rate. Besides “field/current”-related phenomena are still debated, it is well established that the rapid heating can, to some extent, improve the consolidation.

The traditional theoretical framework modelling the heating rate effect on densification is founded on the idea that coarsening and densification possess different activation energies, the first being based

on surface-mediated phenomena, while the latter is mediated by bulk diffusion (either lattice or grain boundary). As such, the relative ratio between coarsening and densification rate decreases as the temperature increases. In this context, fast heating is an effective tool to pass through the low-temperature region where coarsening dominates.

Starting from 2010, another possible mechanism has been proposed [37]. It is based on the concept that rapid consolidation does not leave enough time for the newly formed grain boundaries to relax toward their equilibrium state [38]. Such “more disordered” or “diffuse” grain boundaries are thought to possess diffusion rates different than the conventional ones, hence boosting the densification kinetics.

This concept is the “son” of the grain boundary complexion theory [39]. Originally proposed by Hart in 1968 [40] to explain the embrittlement of metals, the GB complexion theory was later found on a strong theoretical thermodynamic framework and was extended to any class of crystalline materials [40,41]. More recently, their statistical foundations have been discussed by Han, Vitek, and Srolovitz [42] and computational models have been developed and trained to predict them [43].

The complexion represents this “stable grain boundary configuration,” characterized by a local minimum in the free energy landscape (indeed, the GB itself is a defect and is always associated with an excess in free energy, not representing an absolute energy minimum).

When considering a grain boundary, it spontaneously tends to relax towards an equilibrium configuration. Such relaxation can be declined in three different aspects (Fig. 1): (i) a chemical relaxation due to the adsorption of solutes at the grain boundaries to minimize the grain boundary energy (Gibbs’ adsorption); (ii) shape relaxation, forming for instance faceted structures to reduce the grain boundary energy; (ii) a structural relaxation due to the formation of specific atomic arrangement in the grain boundary core, forming “crystal-like base units” repeated in the 2D-space. [39,41,44].

The stability of each complexion depends on the thermodynamic

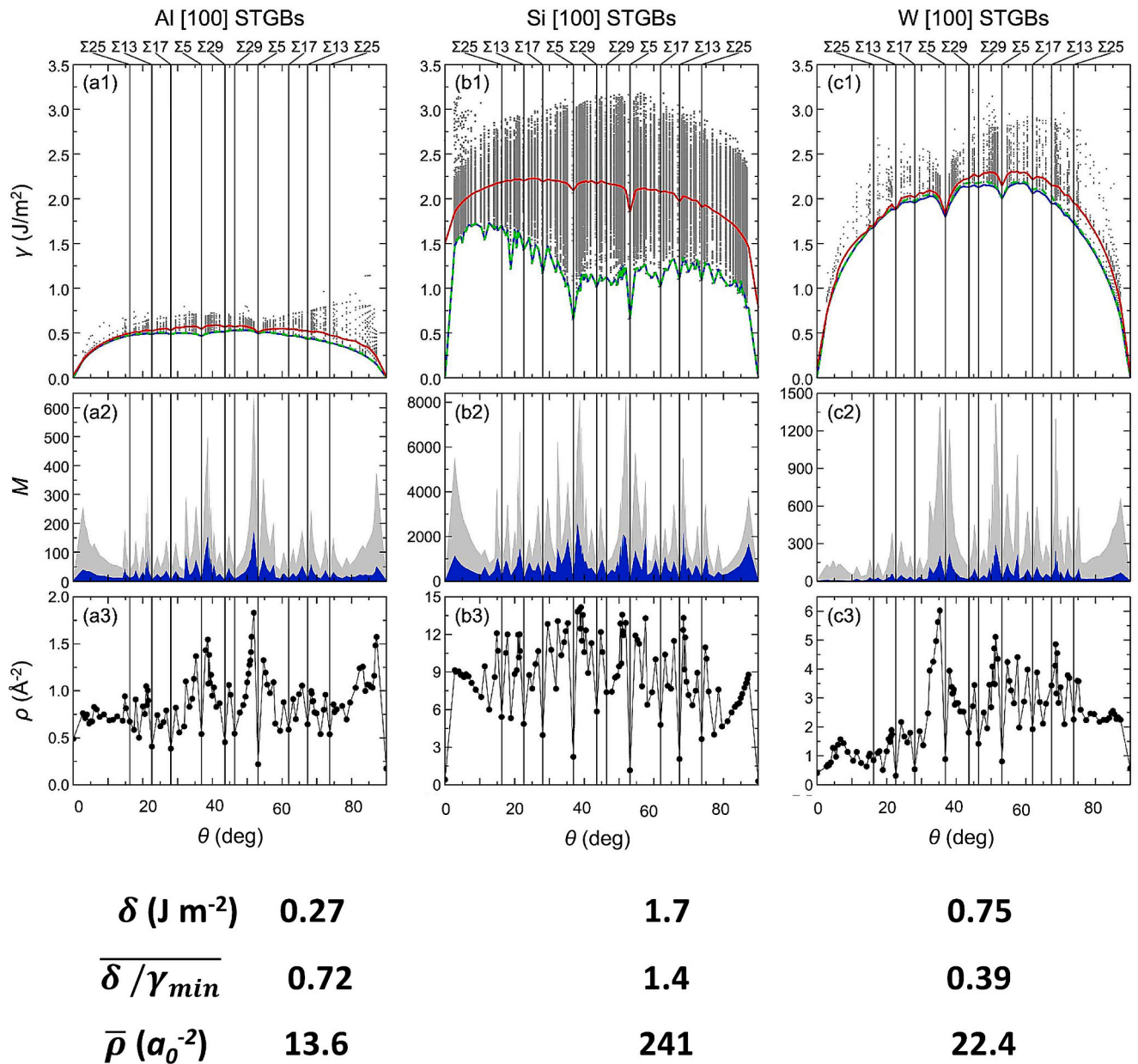


**Fig. 2.** (a1,b1,c1)  $\gamma$ -band for symmetric tilt grain boundaries (STGBs) on the [100] direction for Al, Si, and W as a function of the misorientation angle,  $\theta$ . Gray points identify the different states, the minimum of the band is represented in green, and the red curve represents the average value of  $\gamma$ . Summation symbols denote ensemble averaging over all metastable grain-boundary states at a given misorientation. The bandwidths ( $\delta$ ) and their average value normalized over the minimum of  $\gamma$  ( $\delta/\gamma_{min}$ ) are reported at the bottom of the panel. (a2,b2,c2) The number of states ( $M$ ) is reported in the central row of the panel; degenerate states are highlighted in grey shadow, while the non-degenerate states are in blue. (a3,b3,c3) The density of state is reported on the bottom row of the panel as well as the average density of state ( $\bar{\rho}$ ) over the different misorientations. Reprinted from [42], with permission from Elsevier. (For interpretation of the references to colour in this figure legend, the reader is referred to the web version of this article.)

variables of the system (composition, temperature, and pressure), and complexion transitions do happen at the grain boundary, changing such variables [41]. Actually, TTT-like curves to model the transitions toward the equilibrium GB states have been proposed and verified [45–47] in analogy with the usual 3D phase transitions.

The concept that “stable” GB states exist is directly linked with the idea that metastability can be achieved if the processing conditions do not allow the system to relax. Actually, each grain boundary can exist within a set of different states in polycrystals [48–51], thus developing the so-called  $\gamma$ -band [42], where  $\gamma$  is the GB energy (Fig. 2 a1,b1,c1). Within the  $\gamma$ -band, different states of the same GB are present, producing a distribution in the GB energy within a defined misorientation angle. Indeed, the minimum of the  $\gamma$  band represents the most stable state for a

specific GB.

A bandwidth and a density of states distribution primarily characterize the  $\gamma$ -band. The bandwidth ( $\delta$ ) is defined as the difference between the maximum and minimum grain-boundary energies ( $\gamma_{max(\theta)} - \gamma_{min(\theta)}$ ) and reflects how far the energy distribution extends from the lowest-energy state. Additionally, the normalized bandwidth is the ratio between the average value for  $\gamma_{max(\theta)} - \gamma_{min(\theta)}$  and the average of  $\gamma_{min(\theta)}$  over the different misorientation angles,  $\theta$ . It represents a dimensionless size of the relative energetic distribution of grain-boundary states, allowing direct comparison of metastability across different materials systems. The number of possible states ( $M_{(\theta)}$ , Fig. 2 a2,b2,c2) and density of states ( $\rho_{(\theta)}$ , Fig. 2 a3,b3,c3) for each GB can be extremely large. It is

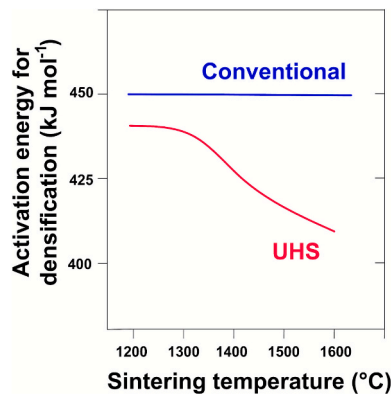


Fig. 3. Activation energy for densification of alumina under conventional and rapid (UHS) sintering conditions as a function of the temperature. Data taken from Guo and Todd [57].

worth stressing that some states are degenerate, thus possessing the same energy (the difference between degenerate and non-degenerate GB states is highlighted in Fig. 2 by the grey and blue shadows). Given the multiplicity of the existing states, it is possible to calculate the grain boundary metastability as Shannon's information entropy ( $S_{(\theta)}$ ) contained in the GB states' multiplicity [42]:

$$S_{(\theta)} = k_b \sum_{i=1}^{M_{(\theta)}} p_{(\theta)}^i \ln(p_{(\theta)}^i) \quad (1)$$

where  $k_b$  is the Boltzmann constant and  $p_{(\theta)}^i$  is the probability associated with the  $i$ -th state in unbiased conditions.

Indeed, at the equilibrium, the system does not lie on a single GB state but on an assembly of states that can be accessed with a probability proportional to the thermal activation ( $\exp(-\gamma^i A_c / k_b T)$ , being  $\gamma^i$  the grain boundary energy of the  $i$ -th state and  $A_c$  is the area in the GB plane of the coincidence lattice site cell [42]). From this perspective, the equilibrium complexion, rather than a single state, can be considered as an equilibrium assembly of states that can be thermally-activated. Obviously, the high-energy states are more accessible and more likely at high temperatures. In the following, the term equilibrium complexion will refer to such a states' assembly rather than a single state.

The characteristic features of the  $\gamma$ -band are material-dependent (Fig. 2). In fact, it has been found that the bandwidth as well as the density of states is substantially larger in covalent compounds than in systems characterized by non-directional metal bonding [42]. See, for instance, the differences between Si, W, and Al in Fig. 2. This has been justified by Han and co-workers based on the idea that a larger number of possible states can be achieved when the bonding is directional [42]. Obviously, a larger bandwidth and a larger number of states reflect a stronger divergence of the GB properties and a larger possibility of grain boundary metastability, enabling GB engineering. While studies in oxide ceramics are still lacking, we can assume that oxides with a substantial covalent contribution to the atomic bonding behave more closely to Si ( $\text{SiO}_2$ ,  $\text{Al}_2\text{O}_3$ ...) while ionic oxides ( $\text{MgO}$ ...) are possibly closer to a directional metal bond.

The atomistic simulations by Bai et al. [52,53] provide supporting evidence that extremely rapid thermal cycles can drive grain boundaries far from equilibrium. During fast heating, the boundaries exhibit a sharp increase in potential energy, indicating the formation of metastable grain boundaries. Subsequent fast cooling causes this metastable state to be "frozen in" because atomic mobility becomes insufficient for structural relaxation, resulting in the retention of non-equilibrium boundary structures at low temperature. In contrast, slower heating and cooling rates enable the boundaries to relax and recover their equilibrium energies.

There has been poor evidence that the sintering process actually

affects the GB complexion till recent days. The first proposal, back in 2010, was based on sole TEM observation of the GBs obtained in alumina by rapid heating, which possessed out-of-equilibrium angles at the triple points and anomalous curvatures [37]. More recently, rapid sintered YSZ, either by flash sintering or flash-SPS, has shown anomalous properties in terms of hardness and electrical response of the grain boundary (specific conductivity/space charge thickness) [54,55]. Moreover, Murakami et al. have shown a substantial reduction of Y segregation close to the grain boundaries of 3YSZ consolidated by UHS, impacting also the phase distribution between tetragonal and cubic zirconia [56]. Also,  $\text{BaZrO}_3$  consolidated by black light sintering (a type of photonic sintering relying mostly on UV light) showed reduced and more "diffuse" grain boundary segregation [18].

In 2025, a careful study of the densification kinetics during UHS by the group of Richard Todd in Oxford showed a variation in the activation energy for densification of alumina when subjected to rapid heating in UHS. Specifically, they measure a decrease in the activation energy from  $460 \text{ kJ mol}^{-1}$  for conventional sintering to  $420 \text{ kJ mol}^{-1}$  for UHS at  $1600^\circ\text{C}$  (Fig. 3) [57]. This result was attributed to the formation of a metastable grain boundary complexion characterized by accelerated diffusion, which explains the exceptional densification kinetics. While the change might seem modest ( $\approx -8.7\%$ ), this translates to an equivalent reduction of the sintering temperature needed to keep the argument of the Arrhenius constant. For ceramics sintering like alumina at  $\approx 1900 \text{ K}$ , such a reduction in the activation energy has the potential of reducing the sintering temperature by more than  $150^\circ\text{C}$ . Remarkably, this effect disappears when the samples were pre-sintered in conventional conditions to densities between 70 and 80%, thus providing a "seed" of equilibrated grain boundaries before the UHS experiment.

It might not be accidental that such results were obtained in alumina, where the covalent character of the bond is close to 50%. Based on the previous analysis, the  $\gamma$ -band in covalent systems is wider and more populated with different states, thus providing a larger spectrum of different possible GB states. As such, an unrelaxed complexion can be substantially different from the equilibrium one, thus enabling non-conventional consolidation kinetics.

### 3. Open questions, scaling laws, and metastability conditions

While it is clear that rapid sintering in high-purity alumina can induce the formation of metastable-high diffusivity GB, the generalization of such a statement to other systems remains an open question. The answer will, in fact, depend on the specific ratio between the relaxation and densification kinetics as well as on the characteristic features of the  $\gamma$ -band, which are material-dependent. As said, the latter is highly dependent on the type of bonding; therefore, it seems more likely that GB metastability can be triggered in covalent/partially covalent ceramics rather than in ionic systems or metals.

Furthermore, it is not clear what the origin of such high diffusivity in alumina is:

- Are the grain boundaries unrelaxed in terms of chemistry? The segregation of dopants at the grain boundary in even high-purity systems might affect the local concentration of point defects and their diffusivity.
- Are the GBs obtained by rapid consolidation more structurally disordered, thus reducing the migration enthalpy of point defects?
- Is the GB shape out of equilibrium, e.g., without the development of faceted structures? Faceting usually occurs to form higher symmetry and lower energy boundaries, thus possibly reducing the local disorder and interacting with the diffusion kinetics. While faceted boundaries can often be observed in alumina [58,59], these are not general phenomena occurring on all the different types of boundaries and temperature ranges. As such, it is hard to think that the absence of faceting is the major origin of the high diffusivity observed in

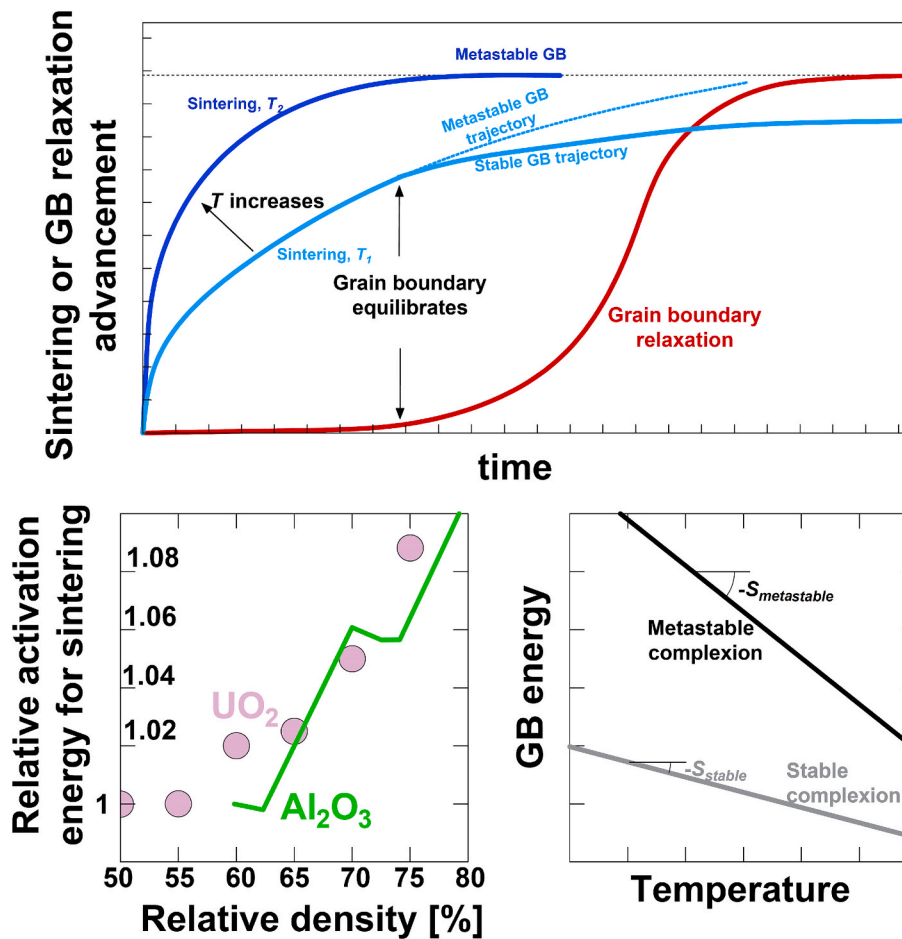


**Fig. 4.** Top panel: Schematic representation of the sintering (blue) and complexion relaxation (red) kinetics. The sintering rate (the slope of the blue curves) is maximum at the beginning and progressively decreases, while the complexion relaxation rate starts from zero (nucleation is needed). The dark blue (high  $T$ ) sintering curves allow densification without relaxation, while in the light blue case, the GB relaxes during sintering, causing a change in the densification kinetics. Bottom left: relative values evolution of the activation energy for sintering in  $\text{UO}_2$  and alumina in the early-intermediate sintering stage (data taken from [63,64]), the increase possibly signals a relaxation of the GB structure. Bottom right: qualitative evolution of the GB energy excess with temperature for a “high entropy” metastable and a “low entropy” stable complexion. (For interpretation of the references to colour in this figure legend, the reader is referred to the web version of this article.)

rapid sintering, as densification involves mass transport through all or, at least, the vast majority of the GB.

Unfortunately, clear microstructural evidence of such a non-equilibrated GB structure is still lacking. The major challenge is related to the fact that real grain boundaries in polycrystalline aggregates are much more complex than the ideal high-symmetry  $\Sigma$  boundaries generally used in HR-TEM studies in bicrystals. Indeed, the presence of  $\Sigma$  GB in polycrystals is possible, but is generally limited. Also, a relatively simple analysis, like the measurement of GB segregations, might be slippery if not supported by a large statistics. Indeed, the GBs can be defined in a vast space with 5 degrees of freedom [60], and each boundary possesses its own chemical structural properties.

### 3.1. Complexion nucleation

*Why do GB not relax within the timeframe of the sintering process?*

The answer is not trivial, as sintering involves transport over the inter-pore distance ( $\approx$ the grain size) of a large portion of the mass of the system, while GB reconstruction is a much more localized phenomenon. A possible explanation could involve the difference in driving forces ( $\gamma_s \Delta A_s \gg \Delta \gamma_{GB} A_{GB}$ ). While it is certainly true that changes in the GB energy are minor when compared with the overall energy involved in sintering, still, they are on the same order of magnitude. More importantly, the formation of a new grain boundary core structure typically

requires a nucleation phenomenon [47,61] that might actually be kinetically-limiting and is crucial for our analysis.

During sintering, the powder system will evolve from surfaces being converted into grain boundaries. In other words, the first interface seed on which the first GB forms falls within a domain substantially different from the one predicted by the equilibrated  $\gamma$ -band. The need for nucleation implies that the equilibrium complexion growth rate ( $\dot{C}_{(t,T)}$ ) at the beginning of the sintering process is equal to zero:

$$\dot{C}_{(t,T)} = \dot{G}_{(t,T)} N_{(t,T)} = \dot{G}_{(t,T)} \int_0^t \dot{N}_{(t,T)} dt \quad (2)$$

with the  $N_{(t,T)}$  the number of nuclei at the time  $t$  of the stable complexion and  $\dot{G}_{(t,T)}$  their growth rate. As the complexion equilibration rate always starts from zero (if no nuclei of the equilibrated complexion are present), then a rapid sintering process might be completed within a timeframe shorter than the relaxation time. Shortening the sintering time is therefore crucial to obtain metastable grain boundaries. This can be achieved by increasing the heating rate, thus quickly reaching high temperatures (see the qualitative sketch in Fig. 4a). Indeed, based on the thermal activation of the sintering process, a temperature increase will always result in shortening of the sintering time ( $t \propto \exp(+Q/kT)$ ,  $Q$  being the activation energy for the diffusion of the slowest species through the fastest path). Note that the process appears to be “self-catalytic”: the growth of metastable boundaries with high diffusivity

accelerates sintering, thus facilitating the conclusion of the densification before a relaxation of the GB.

It is worth stressing that in an ideal case, where the time needed to reach the sintering temperature approaches zero, the linear strain follows:

$$\varepsilon^q = K_{(T)}t \quad (3)$$

with  $q$  being an exponent (usually 2.5–3), depending on the mass transport mechanism[62]. The strain rate has a singularity for  $t \rightarrow 0$ ; therefore, at least in the very early sintering stage, the first grain boundaries are always expected to form out of equilibrium. Hence, it follows that a progressive decrease in the sintering ability is expected as densification proceeds due to the GB relaxation (see the qualitative sketch in Fig. 4a).

Whether or not such a phenomenon could be detected depends on the relaxation kinetics. One can observe that if the GB relaxes quickly at a relatively low temperature where only surface diffusion is activated, then this effect cannot be observed in the strain curve. In other words, when the material starts to shrink, the grain boundaries would already be relaxed. This would result in a constant activation energy for sintering (assuming that it is mediated by GB diffusion) during the entire densification process. However, it is not unusual to find reports in the literature suggesting that the activation energy increases while sintering [63–65]. Often, such variations are modest (a few %, see, for instance, Fig. 4b) in a wide range of densities. Such small variations appear unlikely to be related to the activation of a new diffusion path (e.g., a transition from GB to lattice-mediated densification). The progressive equilibration of the GB toward its equilibrium complexion provides a different perspective on those results that might originate from a change in the GB states. In other words, if the GB relaxes during sintering, one could expect an increase in the activation energy for densification as sketched in Fig. 4b.

We finally remark that while temperature has a monotonic effect in increasing the sintering rate, the same may not occur for the relaxation rate. When the energy excess associated with GB is plotted against temperature, the slope of the curve is the entropy excess at the GB [41]. Intuitively, the unrelaxed boundaries are characterized by a higher entropy excess associated with a more disordered and diffuse structure. As such, the energy difference between the relaxed and unrelaxed complexion decreases when increasing the temperature (see the schematic in Fig. 4c). It is therefore expected that temperature does not have a monotonic effect on the complexion relaxation, including two factors with an opposite effect: the thermal activation (increasing with temperature) and the driving force (decreasing with temperature). Such observation corroborates the idea that increasing the heating rate and the sintering temperature has a positive effect in keeping the system out of equilibrium, higher temperature certainly reducing the sintering time and possibly increasing the relaxation one.

### 3.2. Particle size effect

Considering the chemistry of the material fixed, the formation of metastable GB structure can be considered particle-size dependent. In other words, the same systems with different particle sizes might respond differently to rapid consolidation. This last statement finds some partial experimental confirmation in rapidly sintered YSZ, where fast heating seems less effective in promoting consolidation in coarser systems [25,66,67].

In fact, the sintering rate scales with the particle size ( $a$ ) with a strong power law. Typically, the strain rate is proportional to  $a^{-3}$  or  $a^{-4}$ , for lattice or grain boundary diffusion, respectively. Therefore, considering the temperature constant (isothermal sintering), the time required for sintering substantially decreases with the particle size.

On the other hand, the grain boundary relaxation time should not substantially depend on the particle size in the case of (i) structural

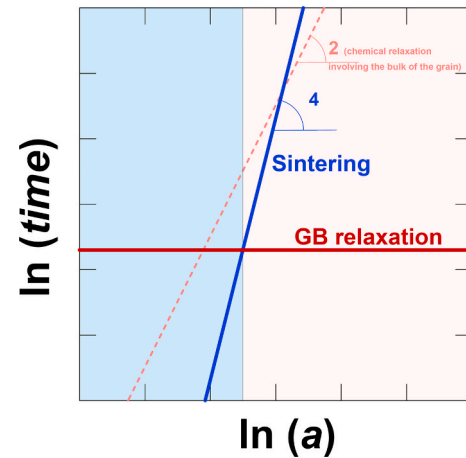


Fig. 5. GB relaxation time compared with the sintering time as a function of the particle size,  $a$ . Note that in the blue-shaded area, sintering is complete in a time shorter than that required to relax the GB. The GB relaxation might follow a different trend (slope = 2) in the case that dopant diffusion from the bulk of the particles is needed. (For interpretation of the references to colour in this figure legend, the reader is referred to the web version of this article.)

relaxation (e.g., some ordering of the GB core); (ii) chemical relaxation involving the diffusion of atoms in the vicinity of the grain boundary; (iii) development of faceted structures. Even in the case that the “chemical relaxation” might require atom diffusion from the bulk of the particle (especially in high-surface area systems or high-purity compounds), then the relaxation time will be proportional only to  $a^2$ , half of the particle size  $a$  being the diffusion distance.

Then, unrelaxed grain boundaries are possible when the sintering time is shorter than the relaxation time, thus leading to:

$$k_{s(T)}a^n < k_{c(T)}a^m \quad (4)$$

Where  $k_{s(T)}$  and  $k_{c(T)}$  a temperature and material-dependent constants modelling the sintering process and complexion relaxation, respectively;  $n$  and  $m$  are characteristic exponents, the former ranging between 3–4, the latter 0–2.

Hence, the sintering without relaxation criterion is:

$$a^{n-m} < k_{c(T)}/k_{s(T)} \quad (5)$$

With  $n-m > 0$ . Therefore, metastability is possible only when the particle size falls below a characteristic temperature and material-dependent threshold (Fig. 5).

There have been extensive studies on the complexion transition during sintering in doped alumina [2] and yttria [45]. The data showed the existence of a complexion transition for Y-doped alumina around 1500°C [2], while Er/Yb-doped yttria showed a transition around 1400°C [45]. Indeed, one can stress that whether or not sintering can be completed below or above this transition can substantially impact the densification/grain growth kinetics by changing the GB properties. On one hand, the change in the complexion can modify the densification rate, on the other, it could also trigger abnormal grain growth [45]. In this regard, any factor changing the consolidation rate and the final sintering temperature (particle size, external pressure...) is crucial for controlling the ceramics' microstructure and properties.

### 3.3. Microstructures

A final question that deserves to be addressed is “How does the grain boundary metastability affect the final microstructure?”. There is no clear answer to this question. However, it is worth noting that the usual claim that “rapid sintering promotes densification over coarsening” might find a new interpretation in the GB metastability context.

Firstly, we notice that the statement refers to surface-mediated

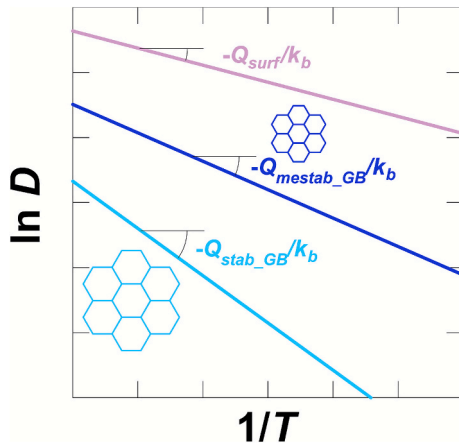


**Fig. 6.** Qualitative representation of the diffusivities,  $D$ , associated with stable and metastable GB and surface diffusion. The slopes correlate with the activation energies. Note that the formation of metastable boundaries increases the relative ratio between densification (GB diffusion) and coarsening (surface diffusion) kinetics, thus facilitating the formation of finer microstructures.

coarsening phenomena active in the early stages and not directly to grain growth in the final sintering stage. The latter is mediated by disconnection slip [68] and has an activation energy substantially larger than the low- $T$  coarsening phenomena [69].

Our traditional understanding of the microstructural evolution is based on the competition between different kinetic phenomena, namely surface diffusion (coarsening) and bulk diffusion (either GB or lattice, causing densification). Fast heating is thought to promote bulk diffusion due to its larger activation energy. The literature is certainly rich in examples of systems where fast heating leads to finer microstructures [24,67,70–73].

Let's consider now that due to a rapid consolidation process, metastable GB with high diffusivity forms. In such a case, we expect a substantial increase in the GB diffusion rate relative to the relaxed complexion (see the schematic in Fig. 6). On the other hand, the coarsening kinetics are unrelated to the densification kinetics and heating rates as the surface of the powder is, in many cases, already equilibrated (e.g., during the calcination process involved in many powder synthesis routes). As such, GB metastability causes an increase in the relative ratio between densification and coarsening, facilitating the formation of finer microstructures [45]. Remarkably, the process appears again “self-catalytic” as reduced coarsening accelerates the consolidation process, thus facilitating a complete densification before

complexion relaxation.

In such a context, the microstructures obtained by fast firing, flash sintering, and UHS can be re-evaluated considering the “microstructural refinement” induced by the GB metastability. We stress that these considerations apply to the competition between surface and bulk diffusion, while no conclusive comments can be made on the grain growth. As a matter of fact, whether and how metastable GB possesses a different growth rate (i.e., different disconnection nucleation and slip) is still unknown, though reasonable.

Scherer et al. reported many pores trapped inside the grains in blacklight-sintered (BS) and UHS-sintered  $\text{BaTiO}_3$ , a feature not present after conventional firing (Fig. 7) [74]. While the UHS atmosphere and temperature might differ from conventional processing, it is worth stressing that the BS occurred in conditions similar to the conventional ones, if one just excludes the heating rate. It is therefore remarkable to observe a very substantial difference in the final microstructures [74]. The origin of the pore-grain boundary separation is the mismatch between the GB mobility and the pore mobility (generally mediated by surface diffusion). Such a result suggests that fast heating enhances the grain boundary migration kinetics over surface diffusion. When grain boundaries move faster than the pores, the pores detach and become enclosed within the grains. At the same time, the reduced pore drag increases grain boundary mobility, promoting further grain growth. Additionally, under rapid heating conditions, pore spheroidization during the early stages of sintering is expected to be largely suppressed due to kinetic constraints.

In summary, these preliminary observations suggest a strong heating-rate-induced acceleration of both densification and grain growth through the formation of metastable GB structures. This argument supports the two-step sintering approach, where a first rapid heating at high temperature (density up to  $\approx 80\%$ ) is followed by a temperature decrease to slowly complete the densification without grain growth [65,75–78]. In fact, if our argument is correct, the GB metastability under fast heating can promote GB migration and facilitate pore breakaway. When this phenomenon happens, then the presence of high diffusivity boundaries does not facilitate the densification anymore, as the pores trapped within the grains can be solely closed by lattice diffusion. Indeed, the pore-GB separation occurs in the final sintering stages, when the porosity transitions by the Rayleigh instability from interconnected (cylinder-like) to isolated (sphere-like). This generally happens at relative densities of about 80–90%. As such, the presence of metastable GB is expected to facilitate densification until this relative density threshold, above which it could even be detrimental. A reduction in the sample temperature, therefore, once a density of about 80% is achieved, can be beneficial.

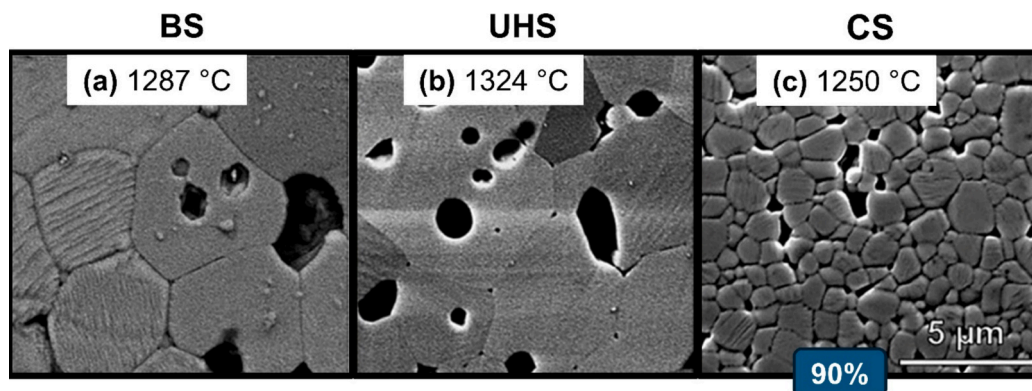


**Fig. 7.** Micrographs illustrating the influence of different sintering techniques on the resulting microstructures. The three rows correspond to distinct processing routes: (a) Blacklight sintering (BS), (b) Ultra-fast high temperature sintering (UHS), and (c) Conventional sintering (CS). Each column represents samples with comparable relative densities of 90%, respectively, obtained from the center of the samples. The sintering temperatures (shown in yellow) are indicated on each micrograph, and the same scale bar applies to all images. Reproduced from [74], with permission from John Wiley and Sons, Copyright 2025. (For interpretation of the references to colour in this figure legend, the reader is referred to the web version of this article.)

#### 4. Conclusions

Ultrafast sintering tools are reshaping the processing science for ceramics. While substantial attention has been focused throughout the last decades on the “microstructural optimization”, the latest scientific results are opening a new, broad perspective. This started from the first experimental observation that the diffusion coefficients at the grain boundaries during rapid sintering are substantially lower than in conventional conditions. The phenomenon has been attributed to the formation, under fast heating, of metastable complexions that can eventually tailor the materials' properties. In this regard, rapid firing offers a new tool for grain boundary engineering via metastability.

The kinetics of the grain boundary relaxation phenomena and densification are discussed, showing that the particle size could play a crucial role in activating metastability. Furthermore, this new perspective allowed us to reassess (i) some general microstructural features occurring in rapid sintering (like grain refinement), (ii) the benefits of two-stage sintering, (iii) the sintering activation energy evolution during densification.

#### Declaration of competing interest

The authors declare that they have no known competing financial interests or personal relationships that could have appeared to influence the work reported in this paper.

#### Data availability

Data will be made available on request.

#### References

- [1] S.J. Dillon, K. Tai, S. Chen, The importance of grain boundary complexions in affecting physical properties of polycrystals, *Curr. Opin. Solid State Mater. Sci.* 20 (2016) 324–335, <https://doi.org/10.1016/j.cossms.2016.06.003>.
- [2] A.R. Krause, P.R. Cantwell, C.J. Marvel, C. Compson, J.M. Rickman, M.P. Harmer, Review of grain boundary complexion engineering: Know your boundaries, *J. Am. Ceram. Soc.* 102 (2019) 778–800, <https://doi.org/10.1111/jace.16045>.
- [3] J.S. Park, Y.-B. Kim, J. An, F.B. Prinz, Oxygen diffusion across the grain boundary in bicrystal yttria stabilized zirconia, *Solid State Commun.* 152 (2012) 2169–2171, <https://doi.org/10.1016/j.ssc.2012.09.019>.
- [4] X. Guo, J. Maier, Grain boundary blocking effect in zirconia: A Schottky barrier analysis, *J. Electrochem. Soc.* 148 (2001) E121, <https://doi.org/10.1149/1.1348267>.
- [5] E. Isotta, S. Jiang, G. Moller, A. Zevalkink, G.J. Snyder, O. Balogun, Microscale imaging of thermal conductivity suppression at grain boundaries, *Adv. Mater.* 35 (2023), <https://doi.org/10.1002/adma.202302777>.
- [6] D. Beretta, N. Neophytou, J.M. Hodges, M.G. Kanatzidis, D. Narducci, M. Martin-Gonzalez, M. Beekman, B. Balke, G. Cerretti, W. Tremel, A. Zevalkink, A.I. Hofmann, C. Müller, B. Dörfling, M. Campoy-Quiles, M. Caironi, Thermolectrics: From history, a window to the future, *Materials Science and Engineering: R: Reports* 138 (2019) 100501, <https://doi.org/10.1016/j.mser.2018.09.001>.
- [7] K.K. Singh, Subrahmanyam, Fast firing of ceramics—a review, *Trans. Indian Ceram. Soc.* 35 (1976) 26–30, <https://doi.org/10.1080/0371750X.1976.10840848>.
- [8] C. Wang, W. Ping, Q. Bai, H. Cui, R. Hensleigh, R. Wang, A.H. Brozena, Z. Xu, J. Dai, Y. Pei, C. Zheng, G. Pastel, J. Gao, X. Wang, H. Wang, J.-C. Zhao, B. Yang, X. (Rayne) Zheng, J. Luo, Y. Mo, B. Dunn, L. Hu, A general method to synthesize and sinter bulk ceramics in seconds, *Science* 368 (2020) (1979) 521–526, <https://doi.org/10.1126/science.aaz7681>.
- [9] T.P. Mishra, S. Wang, C. Lenser, D. Jennings, M. Kindelmann, W. Rheinheimer, C. Broeckmann, M. Bram, O. Guillon, Ultra-fast high-temperature sintering of strontium titanate, *Acta Mater.* 231 (2022) 117918, <https://doi.org/10.1016/j.actamat.2022.117918>.
- [10] M. Cologna, B. Rashkova, R. Raj, Flash sintering of nanograin zirconia in 5 s at 850°C, *J. Am. Ceram. Soc.* 93 (2010) 3556–3559.
- [11] U. Anselmi-Tamburini, J.E. Garay, Z.A. Munir, Fundamental investigations on the spark plasma sintering/synthesis process, *Mater. Sci. Eng. A* 407 (2005) 24–30, <https://doi.org/10.1016/j.msea.2005.06.066>.
- [12] E. Olevsky, L. Froyen, Constitutive modeling of spark-plasma sintering of conductive materials, *Scr. Mater.* 55 (2006) 1175–1178, <https://doi.org/10.1016/j.scriptamat.2006.07.009>.
- [13] E.A. Olevsky, S.M. Rolfing, A.L. Maximenko, Flash (Ultra-Rapid) spark-plasma sintering of silicon carbide, *Sci. Rep.* 6 (2016) 33408, <https://doi.org/10.1038/srep33408>.
- [14] S. Grasso, T.G. Saunders, Spark plasma sintering in a flash, *Am. Ceram. Soc. Bull.* 95 (2016) 32–34.
- [15] C. Manière, G. Lee, E.A. Olevsky, All-materials-inclusive flash spark plasma sintering, *Sci. Rep.* 7 (2017) 15071, <https://doi.org/10.1038/s41598-017-15365-x>.
- [16] S. Grasso, T. Saunders, H. Porwal, O. Cedillos-Barraza, D.D. Jayaseelan, W.E. Lee, M.J. Reece, Flash spark plasma sintering (FSPS) of pure ZrB<sub>2</sub>, *J. Am. Ceram. Soc.* 97 (2014) 2405–2408, <https://doi.org/10.1111/jace.13109>.
- [17] M. Oghbaei, O. Mirzaei, Microwave versus conventional sintering: A review of fundamentals, advantages and applications, *J. Alloys Compd.* 494 (2010) 175–189, <https://doi.org/10.1016/j.jallcom.2010.01.068>.
- [18] J.N. Ebert, D. Jennings, O. Guillon, W. Rheinheimer, Blacklight sintering of BaZrO<sub>3</sub>-based proton conductors, *Scr. Mater.* 256 (2025) 116414, <https://doi.org/10.1016/j.scriptamat.2024.116414>.
- [19] L. Porz, M. Scherer, D. Huhn, L.-M. Heine, S. Britten, L. Rebohle, M. Neubert, M. Brown, P. Lascelles, R. Kitson, D. Rettenwander, L. Fulanovic, E. Bruder, P. Breckner, D. Isaia, T. Frömling, J. Rödel, W. Rheinheimer, Blacklight sintering of ceramics, *Mater. Horiz.* 9 (2022) 1717–1726, <https://doi.org/10.1039/D2MH00177B>.
- [20] L. Karacasulu, C. Manière, C. Vakifahmetoglu, S. Marinel, M. Biesuz, Sintering under high heating rates, *Annu. Rev. Mater. Res.* 55 (2025) 203–230, <https://doi.org/10.1146/annurev-matsci-080323-042441>.
- [21] M. Kermani, C. Hu, S. Grasso, From pit fire to Ultrafast High-temperature Sintering (UHS): A review on ultrarapid consolidation, *Ceram. Int.* 49 (2023) 4017–4029, <https://doi.org/10.1016/j.ceramint.2022.11.091>.
- [22] R. Jiang, E. Torresani, E.A. Olevsky, A review of microstructure evolution and performance improvements in emerging sintering processes under controlled energy input, *J. Mater. Res. Technol.* 39 (2025) 368–391, <https://doi.org/10.1016/j.jmrt.2025.09.129>.
- [23] T. Grippi, A.L. Maximenko, E. Torresani, E.A. Olevsky, Ultra-rapid, pressureless, and optically instrumented manufacturing of high-performance ceramics, *J. Eur. Ceram. Soc.* 46 (2026) 117992, <https://doi.org/10.1016/j.jeurceramsoc.2025.117992>.
- [24] W. Ji, J. Zhang, W. Wang, Z. Fu, R.I. Todd, The microstructural origin of rapid densification in 3YSZ during ultra-fast firing with or without an electric field, *J. Eur. Ceram. Soc.* 40 (2020) 5829–5836, <https://doi.org/10.1016/j.jeurceramsoc.2020.07.027>.
- [25] M. Biesuz, E. De Bona, C. Manière, Fast firing of 3 mol% yttria-stabilized zirconia: On the effect of heating rate on sintering, *J. Am. Ceram. Soc.* 107 (2024) 6596–6606, <https://doi.org/10.1111/jace.19989>.
- [26] A. Kocjan, M. Logar, Z. Shen, The agglomeration, coalescence and sliding of nanoparticles, leading to the rapid sintering of zirconia nanoceramics, *Sci. Rep.* 7 (2017) 2541, <https://doi.org/10.1038/s41598-017-02760-7>.
- [27] Y. Zhang, J. Il Jung, J. Luo, Thermal runaway, flash sintering and asymmetrical microstructural development of ZnO and ZnO-Bi<sub>2</sub>O<sub>3</sub> under direct currents, *Acta Mater.* 94 (2015) 87–100.
- [28] M. Koike, A. Kodaira, T. Tokunaga, T. Yamamoto, Apparent sintering activation energy estimated by master sintering curves for 8 mol% Y<sub>2</sub>O<sub>3</sub>-doped ZrO<sub>2</sub> polycrystals during shrinkage-rate controlled flash sintering, *Mater. Trans.* 64 (2023) MT-M2023048, <https://doi.org/10.2320/matertrans.MT-M2023048>.
- [29] R. Raj, Joule heating during flash-sintering, *J. Eur. Ceram. Soc.* 32 (2012) 2293–2301, <https://doi.org/10.1016/j.jeurceramsoc.2012.02.030>.
- [30] F.R. Monteiro, P.H.F. Oliveira, P.A. Lançon, H.E. de Araújo, D. Pérez-Coll, G. C. Mather, A.L. Chinellato, E.M. de, J.A. Pallone, Enhancing microstructure homogeneity and electrical conductivity in flash-sintered 8YSZ: Impact of electric-current ramp control and thermal insulation, *Mater. Today Commun.* 41 (2024) 110752, <https://doi.org/10.1016/j.mtcomm.2024.110752>.
- [31] Z.A. Munir, U. Anselmi-Tamburini, M. Ohyanagi, The effect of electric field and pressure on the synthesis and consolidation of materials: A review of the spark plasma sintering method, *J. Mater. Sci.* 41 (2006) 763–777, <https://doi.org/10.1007/s10853-006-6555-2>.
- [32] J.M. Frei, U. Anselmi-Tamburini, Z.A. Munir, Current effects on neck growth in the sintering of copper spheres to copper plates by the pulsed electric current method, *J. Appl. Phys.* 101 (2007) 114914, <https://doi.org/10.1063/1.2743885>.
- [33] K.I. Rybakov, E.A. Olevsky, V.E. Semenov, The microwave ponderomotive effect on ceramic sintering, *Scr. Mater.* 66 (2012) 1049–1052, <https://doi.org/10.1016/j.scriptamat.2012.02.043>.
- [34] M. Biesuz, L. Pinter, T. Saunders, M. Reece, J. Binner, V.M. Sglavo, S. Grasso, Investigation of electrochemical, optical and thermal effects during flash sintering of 8YSZ, *Materials* 11 (2018) 1214, <https://doi.org/10.3390/ma11071214>.
- [35] S.K. Jha, H. Charalambous, H. Wang, X.L. Phuah, C. Mead, J. Okasinski, H. Wang, T. Tsakalakos, In-situ observation of oxygen mobility and abnormal lattice expansion in ceria during flash sintering, *Ceram. Int.* 44 (2018) 15362–15369, <https://doi.org/10.1016/j.ceramint.2018.05.186>.
- [36] Y. Dong, H. Wang, I. Chen, Electrical and hydrogen reduction enhances kinetics in doped zirconia and ceria: I. Grain growth study, *J. Am. Ceram. Soc.* 100 (2017) 876–886.
- [37] J. Zhang, F. Meng, R.I. Todd, Z. Fu, The nature of grain boundaries in alumina fabricated by fast sintering, *Scr. Mater.* 62 (2010) 658–661, <https://doi.org/10.1016/j.scriptamat.2010.01.019>.
- [38] W. Ji, B. Parker, S. Falco, J.Y. Zhang, Z.Y. Fu, R.I. Todd, Ultra-fast firing: Effect of heating rate on sintering of 3YSZ, with and without an electric field, *J. Eur. Ceram. Soc.* 37 (2017) 2547–2551.

- [39] P.R. Cantwell, M. Tang, S.J. Dillon, J. Luo, G.S. Rohrer, M.P. Harmer, Grain boundary complexions, *Acta Mater.* 62 (2014) 1–48, <https://doi.org/10.1016/j.actamat.2013.07.037>.
- [40] E.W. Hart, Two-dimensional phase transformation in grain boundaries, *Scr. Metall.* 2 (1968) 179–182, [https://doi.org/10.1016/0036-9748\(68\)90222-6](https://doi.org/10.1016/0036-9748(68)90222-6).
- [41] P.R. Cantwell, T. Prolov, T.J. Rupert, A.R. Krause, C.J. Marvel, G.S. Rohrer, J. M. Rickman, M.P. Harmer, Grain boundary complexion transitions, *Annu. Rev. Mater. Res.* 50 (2020) 465–492, <https://doi.org/10.1146/annurev-matsci-081619-114055>.
- [42] J. Han, V. Vitek, D.J. Srolovitz, Grain-boundary metastability and its statistical properties, *Acta Mater.* 104 (2016) 259–273, <https://doi.org/10.1016/j.actamat.2015.11.035>.
- [43] J. Luo, Computing grain boundary “phase” diagrams, *Interdisciplinary Materials* 2 (2023) 137–160, <https://doi.org/10.1002/idm2.12067>.
- [44] W.D. Kaplan, D. Chatain, P. Wynblatt, W.C. Carter, A review of wetting versus adsorption, complexions, and related phenomena: the rosetta stone of wetting, *J. Mater. Sci.* 48 (2013) 5681–5717, <https://doi.org/10.1007/s10853-013-7462-y>.
- [45] P.R. Cantwell, S. Ma, S.A. Bojarski, G.S. Rohrer, M.P. Harmer, Expanding time–temperature-transformation (TTT) diagrams to interfaces: A new approach for grain boundary engineering, *Acta Mater.* 106 (2016) 78–86, <https://doi.org/10.1016/j.actamat.2016.01.010>.
- [46] C.J. Marvel, A.R. Krause, M.P. Harmer, Effect of Eu-doping and grain boundary plane on complexion transitions in MgAl<sub>2</sub>O<sub>4</sub>, *J. Am. Ceram. Soc.* 104 (2021) 4203–4213, <https://doi.org/10.1111/jace.17831>.
- [47] O. Schumacher, C.J. Marvel, M.N. Kelly, P.R. Cantwell, R.P. Vinci, J.M. Rickman, G.S. Rohrer, M.P. Harmer, Complexion time-temperature-transformation (TTT) diagrams: Opportunities and challenges, *Curr. Opin. Solid State Mater. Sci.* 20 (2016) 316–323, <https://doi.org/10.1016/j.cossms.2016.05.004>.
- [48] Y. Oh, V. Vitek, Structural multiplicity of  $\Sigma = 5(001)$  twist boundaries and interpretation of X-ray diffraction from these boundaries, *Acta Metall.* 34 (1986) 1941–1953, [https://doi.org/10.1016/0001-6160\(86\)90253-1](https://doi.org/10.1016/0001-6160(86)90253-1).
- [49] A. Mishra, S.A. Suresh, S.J. Fensin, N. Mathew, E.M. Kober, Learning from metastable symmetric-tilt grain boundaries using physics-based descriptors, *Phys. Rev. Mater.* 8 (2024) 123605, <https://doi.org/10.1103/PhysRevMaterials.8.123605>.
- [50] M. He, Y. Wang, Y. Fan, Metastable grain boundaries: the roles of structural and chemical disorders in their energetics, non-equilibrium kinetic evolution, and mechanical behaviors, *J. Phys. Condens. Matter* 36 (2024) 343001, <https://doi.org/10.1088/1361-648X/ad4aab>.
- [51] I. Geiger, D. Apelian, X. Pan, P. Cao, J. Luo, T.J. Rupert, Frustrated metastable-to-equilibrium grain boundary structural transition in NbMoTaW due to segregation and chemical complexity, *Acta Mater.* 272 (2024) 119939, <https://doi.org/10.1016/j.actamat.2024.119939>.
- [52] Z. Bai, G.H. Balbus, D.S. Gianola, Y. Fan, Mapping the kinetic evolution of metastable grain boundaries under non-equilibrium processing, *Acta Mater.* 200 (2020) 328–337, <https://doi.org/10.1016/j.actamat.2020.09.013>.
- [53] Z. Bai, A. Misra, Y. Fan, Universal Trend in the dynamic relaxations of tilted metastable grain boundaries during ultrafast thermal cycle, *Mater Res Lett* 10 (2022) 343–351, <https://doi.org/10.1080/21663831.2022.2050957>.
- [54] J.C. M'Peko, J.S.C. Francis, R. Raj, Impedance spectroscopy and dielectric properties of flash versus conventionally sintered yttria-doped zirconia electroceramics viewed at the microstructural level, *J. Am. Ceram. Soc.* 96 (2013) 3760–3767, <https://doi.org/10.1111/jace.12567>.
- [55] T. Hérisson de Beauvoir, Z. Ghomari, G. Chevallier, A. Flaureau, A. Weibel, C. Elissalde, F. Mauvy, R. Chaim, C. Estournès, Flash Spark Plasma Sintering of 3YSZ: Modified sintering pathway and impact on grain boundary formation, *J. Eur. Ceram. Soc.* 41 (2021) 7762–7770, <https://doi.org/10.1016/j.jeurceramsoc.2021.08.013>.
- [56] R. Murakami, B. Feng, K. Matsui, S. Kondo, N. Shibata, Y. Ikuhara, Fabrication of 3YSZ with single tetragonal phase by ultrafast high-temperature sintering, *Ceram. Int.* 50 (2024) 37308–37313, <https://doi.org/10.1016/j.ceramint.2024.04.118>.
- [57] Z. Guo, R.I. Todd, Acceleration of grain boundary diffusion during ultra-fast firing (UHS) of alumina powder compacts, *Acta Mater.* 282 (2025) 120471, <https://doi.org/10.1016/j.actamat.2024.120471>.
- [58] S. Dillon, M. Harmer, Multiple grain boundary transitions in ceramics: A case study of alumina, *Acta Mater.* 55 (2007) 5247–5254, <https://doi.org/10.1016/j.actamat.2007.04.051>.
- [59] B.B. Straumal, O.A. Kogtenkova, A.S. Gornakova, V.G. Sursaeva, B. Baretzky, Review: grain boundary faceting–roughening phenomena, *J. Mater. Sci.* 51 (2016) 382–404, <https://doi.org/10.1007/s10853-015-9341-1>.
- [60] J. Han, S.L. Thomas, D.J. Srolovitz, Grain-boundary kinetics: A unified approach, *Prog. Mater. Sci.* 98 (2018) 386–476, <https://doi.org/10.1016/j.pmatsci.2018.05.004>.
- [61] C.J. Marvel, C. Riedel, W.E. Frazier, A.D. Rollett, J.M. Rickman, M.P. Harmer, Relating the kinetics of grain-boundary complexion transitions and abnormal grain growth: A Monte Carlo time-temperature-transformation approach, *Acta Mater.* 239 (2022) 118262, <https://doi.org/10.1016/j.actamat.2022.118262>.
- [62] M.N. Rahaman, *Ceramic processing and sintering*, Marcel Dekker, New York, USA, 1996.
- [63] L. Balice, M. Cologna, F. Audubert, J.-L. Hazemann, Densification mechanisms of UO<sub>2</sub> consolidated by spark plasma sintering, *J. Eur. Ceram. Soc.* 41 (2021) 719–728, <https://doi.org/10.1016/j.jeurceramsoc.2020.07.002>.
- [64] T. Frueh, I.O. Ozer, S.F. Poterala, H. Lee, E.R. Kupp, C. Compson, J. Atria, G. L. Messing, A critique of master sintering curve analysis, *J. Eur. Ceram. Soc.* 38 (2018) 1030–1037, <https://doi.org/10.1016/j.jeurceramsoc.2017.12.025>.
- [65] J. Yang, L. Lei, J. Zhang, Preparation of alumina ceramics via a two-step sintering process, *Materials* 18 (2025) 1789, <https://doi.org/10.3390/ma18081789>.
- [66] J. Dong, V. Pouchly, M. Biesuz, V. Tyrpek, M. Vilémová, M. Kermani, M. Reece, C. Hu, S. Grasso, Thermally-insulated ultra-fast high temperature sintering (UHS) of zirconia: A master sintering curve analysis, *Scr. Mater.* 203 (2021) 114076, <https://doi.org/10.1016/j.scriptamat.2021.114076>.
- [67] M. Biesuz, T.H. de Beauvoir, E. De Bona, M. Cassetta, C. Manière, V.M. Sglavo, C. Estournès, Ultrafast high-temperature sintering (UHS) vs. conventional sintering of 3YSZ: microstructure and properties, *J. Eur. Ceram. Soc.* 44 (2024) 4741–4750, <https://doi.org/10.1016/j.jeurceramsoc.2024.01.064>.
- [68] K. Chen, J. Han, D.J. Srolovitz, On the temperature dependence of grain boundary mobility, *Acta Mater.* 194 (2020) 412–421, <https://doi.org/10.1016/j.actamat.2020.04.057>.
- [69] R. Chaim, Activation energy and grain growth in nanocrystalline Y-TZP ceramics, *Mater. Sci. Eng. A* 486 (2008) 439–446, <https://doi.org/10.1016/j.msea.2007.09.022>.
- [70] V. Esposito, E. Traversa, Design of electroceramics for solid oxides fuel cell applications: Playing with ceria, *J. Am. Ceram. Soc.* 91 (2008) 1037–1051, <https://doi.org/10.1111/j.1551-2916.2008.02347.x>.
- [71] M. Biesuz, L. Spiridigliozzi, M. Frasnelli, G. Dell’Aglia, V.M.V.M. Sglavo, Rapid densification of Samarium-doped Ceria ceramic with nanometric grain size at 900–1100 °C, *Mater. Lett.* 190 (2017) 17–19, <https://doi.org/10.1016/j.matlet.2016.12.132>.
- [72] E. Zapata-Solvas, D. Gómez-García, A. Domínguez-Rodríguez, R.I. Todd, Ultra-fast and energy-efficient sintering of ceramics by electric current concentration, *Sci. Rep.* 5 (2015) 8513, <https://doi.org/10.1038/srep08513>.
- [73] Y. Zhang, J. Nie, J.M. Chan, J. Luo, Probing the densification mechanisms during flash sintering of ZnO, *Acta Mater.* 125 (2017) 465–475.
- [74] M. Scherer, Z. Guo, L. Fulanović, R.I. Todd, J. Rödel, Sintering at extreme rates: A comparative study between blacklight and ultrafast high-temperature sintering, *J. Am. Ceram. Soc.* 108 (2025), <https://doi.org/10.1111/jace.70085>.
- [75] J. Nie, Y. Zhang, J.M. Chan, S. Jiang, R. Huang, J. Luo, Two-step flash sintering of ZnO: Fast densification with suppressed grain growth, *Scr. Mater.* 141 (2017) 6–9, <https://doi.org/10.1016/j.scriptamat.2017.07.015>.
- [76] N.J. Lóh, L. Simão, C.A. Faller, A. De Noni, O.R.K. Montedo, A review of two-step sintering for ceramics, *Ceram. Int.* 42 (2016) 12556–12572, <https://doi.org/10.1016/j.ceramint.2016.05.065>.
- [77] I.-W. Chen, X.-H. Wang, Sintering dense nanocrystalline ceramics without final-stage grain growth, *Nature* 404 (2000) 168–171, <https://doi.org/10.1038/350004548>.
- [78] I.R. Lavagnini, J.V. Campos, E.M.J.A. Pallone, Microstructure evaluation of 3YSZ sintered by two-step flash sintering, *Ceram. Int.* 47 (2021) 21618–21624, <https://doi.org/10.1016/j.ceramint.2021.04.174>.